

HIGH-RESOLUTION SOIL MOISTURE MAPPING IN AFGHANISTAN

Jan M.H. Hendrickx¹, J. Bruce J. Harrison and Brian Borchers
New Mexico Tech, Socorro, NM 87801

Julie R. Kelley, Stacy Howington and Jerry Ballard
Coastal and Hydraulics Laboratory, Engineer Research and Development Center
Army Corps of Engineers, Vicksburg, MS 39180-6199

ABSTRACT

Soil moisture conditions have an impact upon virtually all aspects of Army activities and are increasingly affecting its systems and operations. Soil moisture conditions affect operational mobility, detection of landmines and unexploded ordnance, natural material penetration/excavation, military engineering activities, blowing dust and sand, watershed responses, and flooding. This study further explores a method for high-resolution (2.7 m) soil moisture mapping using remote satellite optical imagery that is readily available from Landsat and QuickBird. The soil moisture estimations are needed for the evaluation of IED sensors using the Countermine Simulation Testbed in regions where access is difficult or impossible. The method has been tested in Helmand Province, Afghanistan, using a Landsat7 image and a QuickBird image of April 23 and 24, 2009, respectively. In previous work it was found that Landsat soil moisture can be predicted from the visual and near infra-red Landsat bands 1-4. Since QuickBird bands 1-4 are almost identical to Landsat bands 1-4, a Landsat soil moisture map can be downscaled using QuickBird bands 1-4. However, using this global approach for downscaling from Landsat to QuickBird scale yielded a small number of pixels with erroneous soil moisture values. Therefore, the objective of this study is to examine how the quality of the downscaled soil moisture maps can be improved by using a data stratification approach for the development of downscaling regression equations for each landscape class. It was found that stratification results in a reliable downscaled soil moisture map with a spatial resolution of 2.7 m.

Keywords: soil moisture, Landsat, QuickBird, IED, Helmand, Afghanistan

1. INTRODUCTION

Soil moisture conditions have an impact upon virtually all aspects of Army activities and are increasingly affecting its systems and operations. Soil moisture conditions affect operational mobility^[1], detection of landmines and unexploded ordnance^[2-10], military engineering activities, blowing dust and sand, watershed responses^[11-15], and flooding^[16, 17]. Soil moisture also determines near-surface atmospheric conditions and the partition of incoming solar and long-wave radiation between sensible and latent heat fluxes^[18, 19]. Atmospheric turbulence can hamper the performance of optical and infrared sensors as well as acoustic detection systems. The lack of reliable soil moisture maps for weather prediction models can result in significant over- or under-estimation of surface evaporation which results in great uncertainty for the predictions of cloud cover, precipitation, air and soil temperature, and humidity^[20]. Finally, soil moisture is a critical factor for prediction of the strength of aircraft landing sites^[21] and of helicopter brownout conditions^[22].

Spatial scales of interest range from the theater scale (maneuverability), watershed scale (river crossing), field scale (trafficability), and meter to sub-meter scale (IED and land mine detection). Soil moisture at each of these scales is a very dynamic variable subject to rapid changes in time as well as with depth and space. Soil moisture fields are not continuous but are full of discontinuities caused by many factors, including: strong precipitation gradients, snowfall redistribution, topographical divides, slope-aspect, land-use, differences in soil hydraulic properties, fluvial/aeolian

¹ JanHendrickxNMT@gmail.com; phone: 575-835-5892; 801 LeRoy Place, NMT/MSEC 240, Socorro NM 87801.

deposition, human intervention (irrigation, drainage, flooding), and vegetation cover. The existence of discontinuities in soil moisture fields and their temporal variability make it difficult to use statistical interpolation techniques based on a limited number of point measurements for the generation of high resolution soil moisture maps. Accurate predictions of regional soil moisture distributions require direct remote sensing observations that capture discontinuities in soil moisture fields.

Near real time information on the spatial distribution of soil moisture will result in (i) significant improvements in battlefield decision making capabilities for mobility and trafficability modeling^[23, 24], (ii) improved prediction of performance of landmine and IED sensors^[4, 10, 25, 26] as well as of other electromagnetic and thermal sensors employed by the Army, and (iii) greatly improved assimilation of soil moisture data at different scales into hydrologic models for the prediction of watershed responses and flooding^[27]. Building on earlier soil moisture mapping research by our team^[28, 29] using Landsat imagery at 30 m resolution, the objective of this study is to improve a method for soil moisture mapping by downscaling the Landsat soil moisture product using QuickBird optical imagery with pixel size of 2.7 m^[30].

The ultimate goal of this study is to develop a method for meter scale soil moisture retrieval for initialization of the ERDC Countermine Simulation Testbed at sites where no ground measurements are available such as Helmand Province in southern Afghanistan^[30-33].

2. EVAPORATIVE FRACTION METHOD FOR SOIL MOISTURE MAPPING

The evaporative fraction method is based on the long-known relationship between root zone soil moisture and the partition of incoming short and long-wave radiation between sensible and latent heat fluxes^[34-37]. The method became feasible only recently after development and validation of algorithms to derive reliable estimates of the fluxes of the energy balance from remotely sensed optical and thermal imagery^[28, 38-45].

In many agro-hydrological studies root zone soil moisture is used to reduce potential evapotranspiration to actual evapotranspiration^[46-50]. When the soil is wet, most of the available energy (net radiation minus soil heat flux) is used for evapotranspiration or latent heat flux (λE) and almost no energy is left for sensible heat flux (H). When the soil is dry, most of the available energy is used to heat the soil so that latent heat flux (evapotranspiration) becomes small. One way to express this partitioning of radiant energy is the evaporative fraction (Λ) that is defined as the latent heat flux divided by the net available energy^[51, 52]. The net available energy equals net radiation (R_n) minus the soil heat flux (G).

$$\Lambda = \frac{\lambda E}{\lambda E + H} = \frac{\lambda E}{R_n - G} \quad [1]$$

The energy partitioning calculated with the evaporative fraction is primarily related to the soil moisture content^[53]. Using *in situ* root zone soil moisture measurements and validated evaporative fraction data from the Surface Energy Balance for Algorithm for Land (SEBAL) obtained during field experiments in Kansas and Spain, the following empirical relationship was determined^[40]:

$$S = \frac{\theta}{\theta_{sat}} = e^{\frac{\Lambda-1}{0.42}} \quad [2]$$

where S is degree of saturation, θ is volumetric water content, and θ_s is volumetric water content at saturation. Eq. [2] was derived from soil moisture measurements obtained on grazed and un-grazed grassland in Kansas on alluvial soils and loess^[54] as well as from rainfed (vineyard, barley, wheat) and irrigated crops (maize, alfalfa) in Central Spain on sandy loams^[39, 55]. Using evaporative fraction (Λ) estimates obtained from the remote sensing algorithms Surface Energy Balance Algorithms for Land (SEBAL)^[45] or Mapping EvapoTranspiration at High Resolution with Internalized Calibration (METRIC)^[56] Eq. [2] can be used to obtain estimates of degree of saturation (S) in the root zone from optical satellite imagery such as Landsat and MODIS.

A validation of Eq. [2] was conducted using soil moisture data from irrigated fields in Pakistan and Mexico. Equation [2] predicted soil moisture with a root mean square error of $0.05 \text{ cm}^3 \text{ cm}^{-3}$; the error is less than $0.07 \text{ cm}^3 \text{ cm}^{-3}$ in 90% of cases. Given the wide range of conditions used to derive and to validate Eq. [2] it was concluded that Eq. [2] is minimally affected by vegetation type or soil type and may have general applicability^[38].

Figure 1 presents a Landsat7 image covering a typical area of approximately $16 \times 12 \text{ km}$ in Helmand Province (Afghanistan) on April 23, 2009. This area is taken from the center of a Landsat7 image (Path 155, Row 38) that doesn't contain any stripes. The pixel size is $30 \times 30 \text{ m}$. This image is converted into a soil moisture map by first calculating the

latent and sensible heat fluxes using METRIC and then the degree of soil moisture saturation using Eq. [2] (Figure 2). Similar soil moisture maps have been validated quantitatively^[38, 40, 57] as well as qualitatively^[28, 29].

3. PREVIOUS RESEARCH: DOWNSCALING LANDSAT SCALE SOIL MOISTURE MAP TO QUICKBIRD SCALE WITHOUT STRATIFICATION

The soil moisture map in Fig. 2 has a spatial resolution of 30 m that is often too coarse for the initialization of the Countermine Simulation Testbed since the typical dimension of an IED will be on the order of one meter or less. Therefore, it is necessary to downscale the Landsat soil moisture map. A Landsat image has 3 visual bands (1, 2, and 3), one near-infrared band (4), two mid-infrared bands (5, 7) and one thermal infrared band (6). All these bands are needed to implement METRIC for evaluation of the evaporative fraction and soil moisture using energy balance physics. Of special importance is the thermal band 6 since without it METRIC cannot be employed. QuickBird has only four bands: three visual (1, 2, 3) and one near-infrared (4) that are almost identical to Landsat bands 1-4. Since QuickBird has no thermal infra-red band it is impossible to derive a soil moisture map from QuickBird imagery using METRIC. Instead the challenge is to predict soil moisture using only bands 1-4.

In previous research we found that Landsat soil moisture can be predicted from the digital values of Landsat bands 1-4 using a simple linear regression equation. Figure 3 shows the excellent agreement between METRIC soil moisture and the soil moisture predicted from Landsat bands 1-4. It is “proof of concept” that soil moisture can be predicted from the digital values of Landsat bands 1, 2, 3, and 4 and, therefore, most likely also from the digital values of bands 1, 2, 3, and 4 of QuickBird imagery. Indeed, using the same regression equation with the digital values of QuickBird bands 1-4 (QuickBird image of April 24, 2009) resulted in quite reliable soil moisture predictions in most of our study area but in some locations the soil moisture predictions were not correct^[30]. For example, dry hot asphalt roads showed elevated moisture contents while moist cool sandbars in the river were predicted to have no soil moisture at all. Although promising, such a result is not acceptable for an operational soil moisture map at the m-scale. Therefore, the objective of this study is to test whether the downscaled soil moisture map can be improved by first classifying the study area in different landscape units and then to develop a regression equation for each of those units.

4. DOWNSCALING LANDSAT SCALE SOIL MOISTURE MAP TO QUICKBIRD SCALE WITH STRATIFICATION

There are many different ways to stratify an area into different landscape units. One proven method is to classify the geo-morphological units on the basis of landscape features observed on high-resolution aerial or satellite imagery^[58]. Another method is to use unsupervised classification algorithms available in most remote sensing processing software^[59]. We have work in progress with both approaches but in this study we report on the latter. Using ERDAS Imagine 2011 we classified our study areas in ten different classes based on the Normalized Difference Vegetation Index (NDVI), albedo and surface temperature obtained from the Landsat image applying METRIC as well as the digital values of bands 1-4 of the QuickBird image. The spatial scale of the classified image is 2.7 m equal to the spatial scale of the QuickBird image.

As expected the landscape classes show a similar pattern (Fig. 4) to those shown on the original false color Landsat image (Fig. 1) and the Landsat soil moisture image (Fig. 2). However, the details of the landscape classification map shown over a 1300×800 m area (Fig. 5) indicate that changes in class do also occur within one field and over short distances and are not always related to the overall patterns shown on Figure 4. In this respect, the unsupervised classification approach deviates from a traditional geo-morphological landscape classification map since the unsupervised classification map seems to identify with high accuracy all anomalies within a traditional geo-morphological landscape unit.

Next, we determined for each unit the most relevant regression equation for the prediction of the soil moisture status on each 2.7×2.7 m pixel from Landsat bands 1-4, NDVI, albedo and surface temperature from METRIC as well as the digital values of QuickBird bands 1-4. The regression equations were all significant at a level of less than 0.0001 and their R^2 varied between 77 and 83 percent which indicates that they explain a major part of the variability within each landscape class. We do not report any regression equation since they are all site and time specific and, therefore, cannot be used for any other time or site.

The final step is to plot and regress the Quickbird predicted soil moisture (PSM) with stratification against the Landsat soil moisture (SM). Figure 6 clearly demonstrates that the stratification greatly improves the downscaled soil

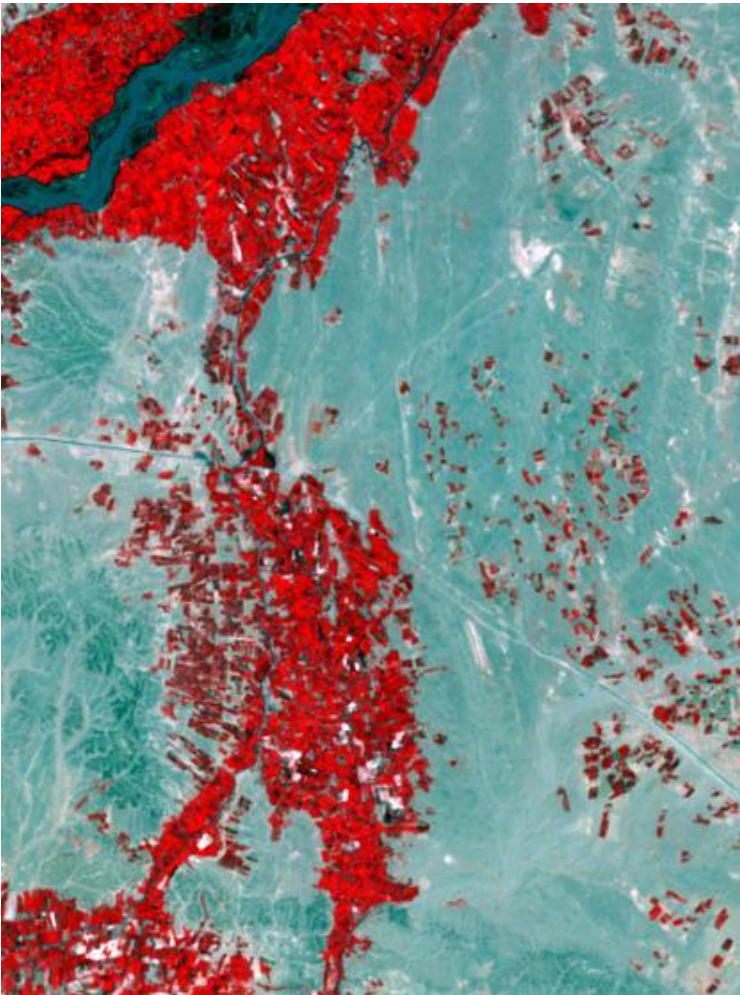


Figure 1. Landsat7 Image on April 23, 2009, in false colors. Vegetation is colored red. Spatial resolution is 30 m pixel size. Image area is about 16x12 km. The area is located in the center of the image that doesn't contain stripes.

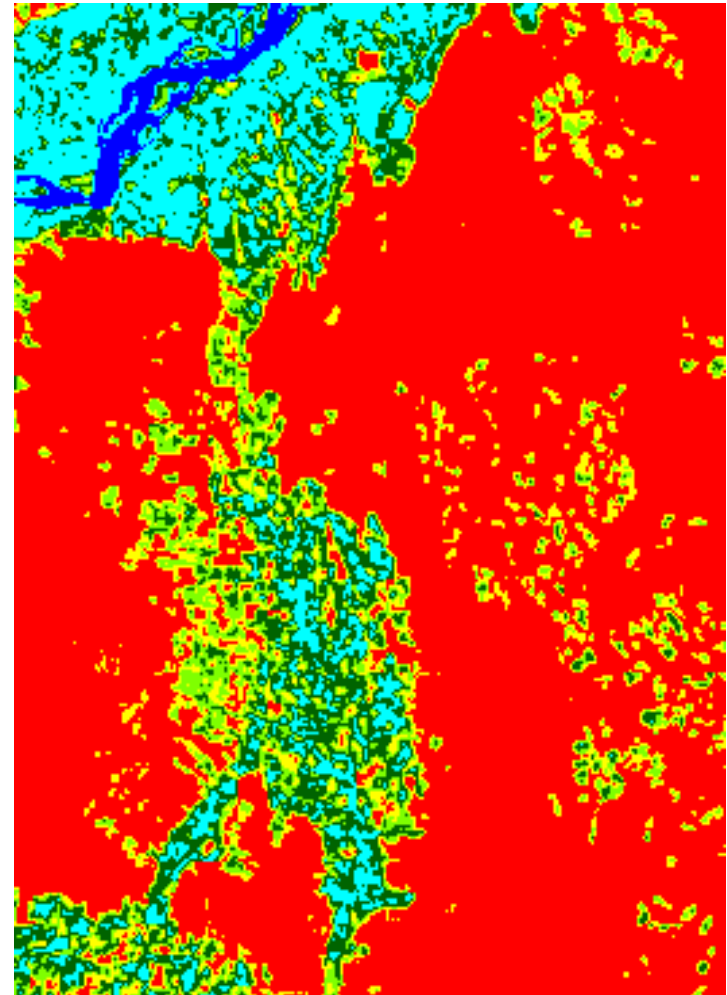


Figure 2. Landsat7 Soil Moisture Map on April 23, 2009. Spatial resolution is 30 m pixel size. Image area is about 16x12 km. Soil moisture expressed as degree of soil saturation: 0.0-0.2 red; 0.2-0.4 yellow; 0.4-0.6 light green; 0.6-0.8 green; 0.8-1.0 light blue. Water is colored blue. This map is slightly different from the one presented in 2010^[30].

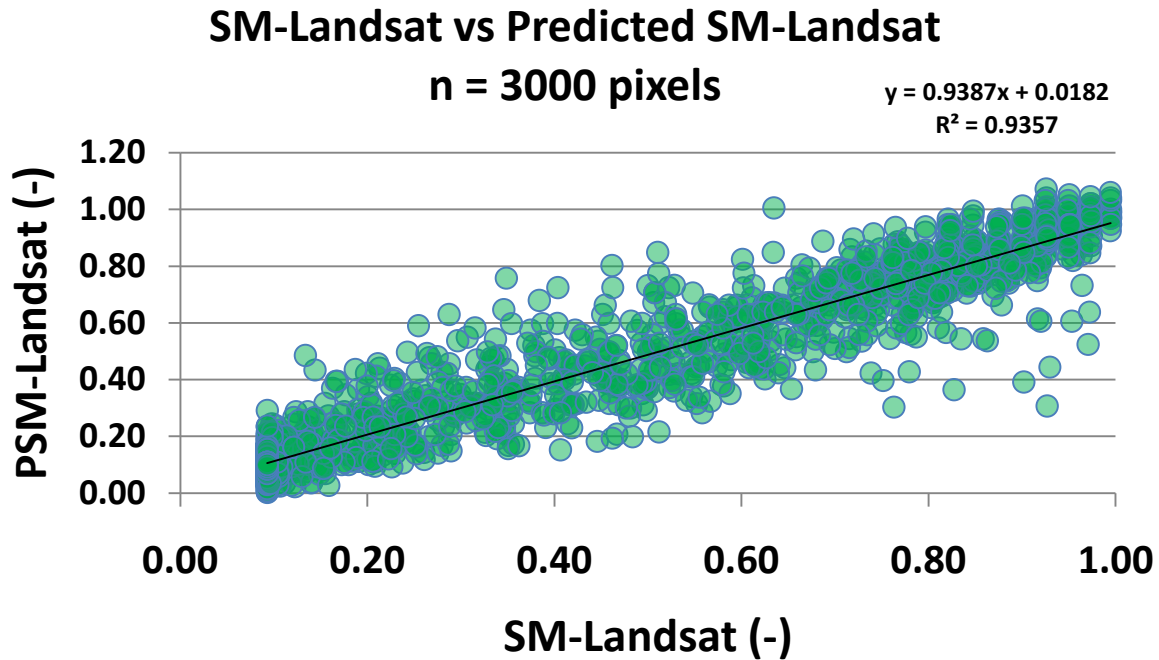


Figure 3. Regression between Landsat Soil Moisture (SM) from METRIC and its prediction (PSM) using Landsat bands 1-4. The cut-off at soil moisture of 0.09 is an artifact of Eq. [2] that yields a minimum soil moisture degree value at 0.09. The number of outliers is very small considering that this figure represents 3,000 pixels.

moisture map as compared to the global approach with only one regression equation that we used before (see Fig. 8 of Hendrickx et al.^[30]).

5. INSPECTION OF QUICKBIRD SCALE SOIL MOISTURE MAP

A strong correlation and significant regression does exist between the METRIC Landsat scale soil moisture map and the downscaled Quickbird soil moisture map (Fig. 6) but the final proof of the quality of the downscaled map using stratification is found by comparison of the stratification with the global downscaling approach. We will do this by inspection of the same two 3×3 km areas reported on by Hendrickx et al. in 2010^[30].

The first area covers contiguous irrigated fields interspersed with almost bare dry lands; the most important feature for our inspection is an asphalt road going from East to West. Figure 7 shows the QuickBird image, Landsat soil moisture map and the downscaled soil moisture maps using, respectively, the global and stratification approach. Whereas the dry hot asphalt road contains erroneous elevated moisture contents on the global approach image, it is almost dry on the stratification approach image.

The second area covers contiguous irrigated field crossed by a wide river with sandbanks and a small village on the left side of the image. Figure 8 shows the QuickBird image, Landsat soil moisture map and the downscaled soil moisture maps using, respectively, the global and stratification approach. As observed in the first area there exists generally good agreement between the Landsat and Quickbird soil moisture maps in the irrigated areas. In this area the most important feature for inspection is the sandbank in the river. Using the global approach the sandbank is covered with dry or slightly moist pixels while the Landsat soil moisture map clearly indicates elevated soil moisture levels on the sandbank. The stratification approach image contains much more realistic soil moisture values that agree reasonably well with the Landsat soil moisture map. Of interest is also the village: whereas the Landsat soil moisture map shows a generally elevated soil moisture over the entire village, the

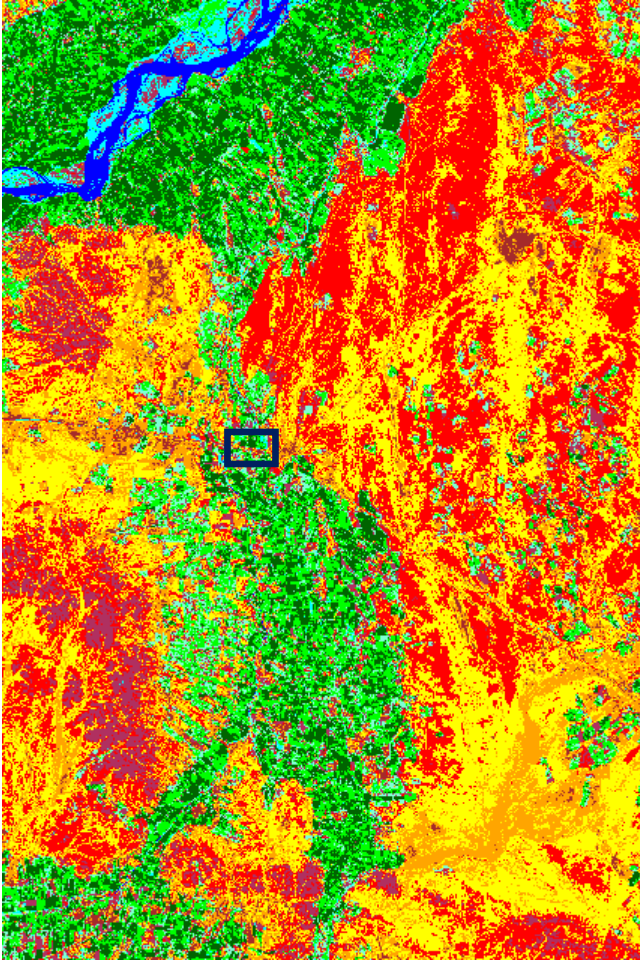


Figure 4. Landscape classification maps with ten different classes each with a different color. The classification is based on NDVI, albedo and surface temperature from the Landsat image and the four Quickbird bands 1-4. Spatial resolution is 2.7 m pixel size. Image area is about 16x12 km. The black rectangle represents the area shown in Figure 5.

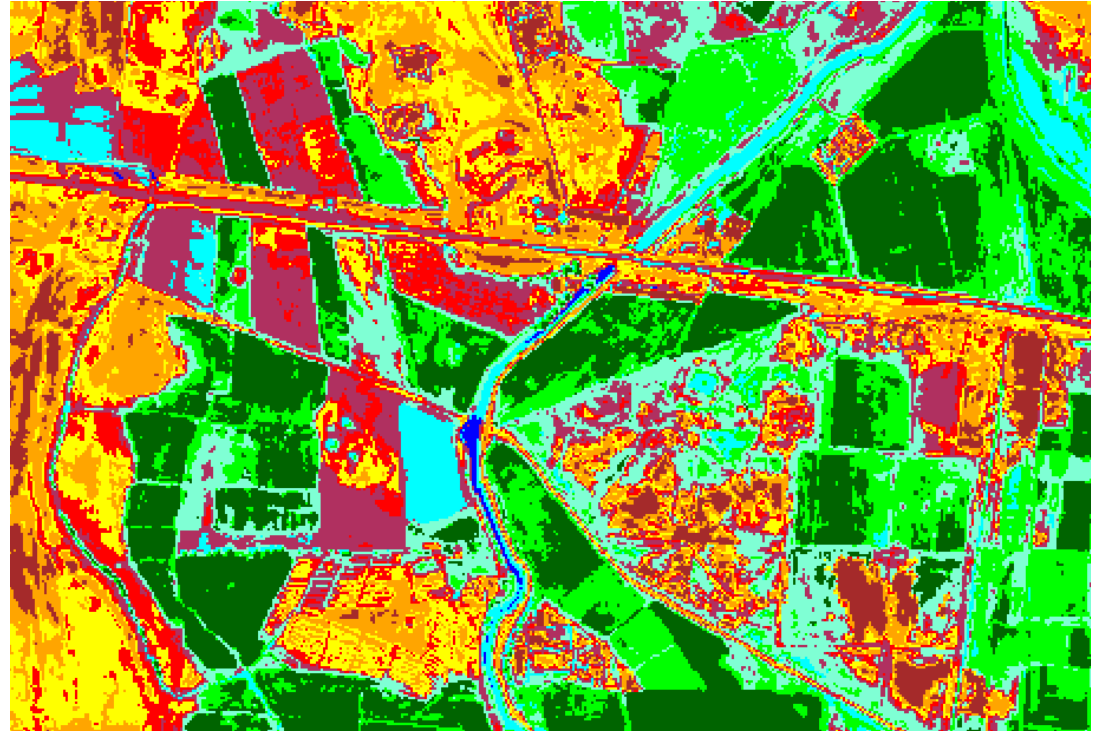


Figure 5. Detail of the landscape classification map covering about 1300x800 m inside the black rectangle in Figure 4. The map shows that several landscape classes can occur within one field and/or over small distances. Each landscape class has its own regression equation for downscaling soil moisture from 30 m to 2.7 m scale. The water class is colored blue.

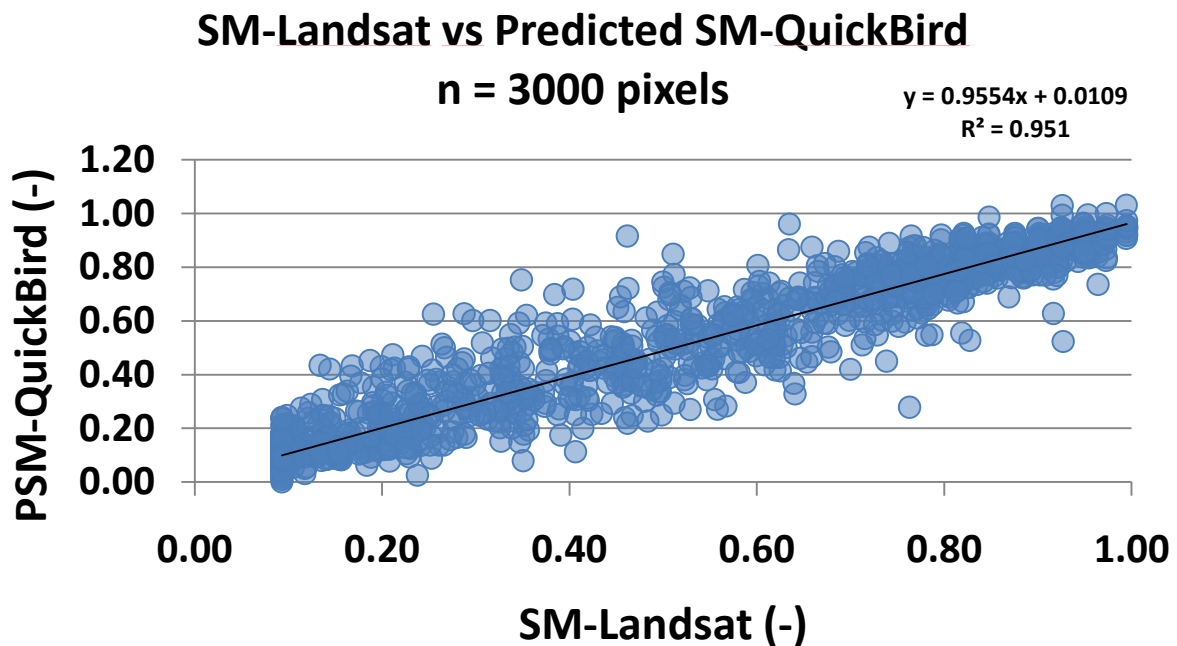


Figure 6. Regression between Landsat Soil Moisture (SM) from METRIC and its prediction (PSM) using Landsat bands 1-4, NDVI, albedo and surface temperature from METRIC as well as QuickBird bands 1-4; for each landscape class a different regression equation was developed. The cut-off at soil moisture of 0.09 is an artifact of Eq. [2] that yields a minimum soil moisture degree value at 0.09. The number of outliers is very small considering that this figure represents 3,000 pixels.

stratification approach images indicates the location of completely dry pixels as can be expected in the village environment. The elevated soil moisture pixels in the village on the Landsat soil moisture map may be caused by the effect of the shadows of the village structures that will result in somewhat lower surface temperatures and, therefore, slightly erroneous soil moisture prediction.

Overall the quality of the downscaled QuickBird soil moisture map has improved considerably as compared to the global approach^[30] (Figs. 7 and 8). It captures well all the features observed on the Landsat soil moisture map at a high spatial resolution. Therefore, this study demonstrates that (i) stratification is an effective procedure for the improvement of the quality of downscaled soil moisture maps and (ii) combining Landsat soil moisture maps at 30 m scale with aerial or satellite imagery with visual and near infrared bands at the m-scale will result in reliable soil moisture maps at the m-scale.

6. CONCLUSIONS AND FUTURE WORK

Two major conclusions result from this study and a previous one^[30]: 1. METRIC derived root zone soil moisture can be predicted from reflectance of the three visual and one near-infrared band of Landsat and Quickbird operational optical satellite images; 2. Due to differences in soil types and land covers one regression equation is not sufficient for the reliable estimation of soil moisture over an entire image but when regression equations are developed for each landscape unit in the image a reliable soil moisture image is produced at m-scale resolution.

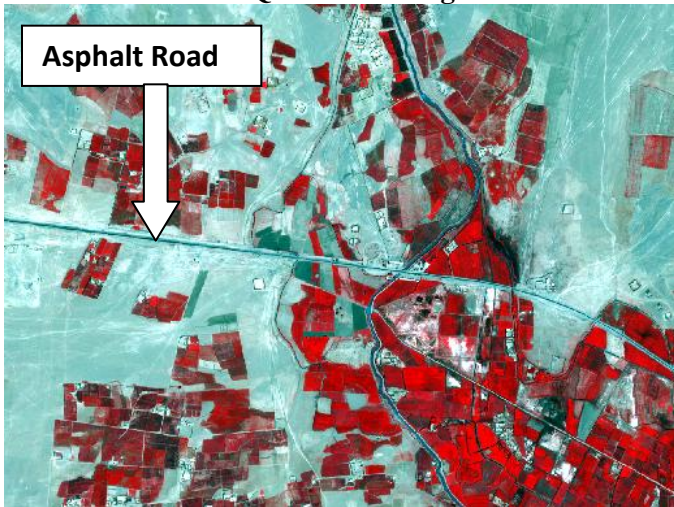
Our results are irrefutable evidence that reliable m-scale soil moisture maps can be produced using existing algorithms such as METRIC and SEBAL with Landsat imagery at the 30 m scale together with simultaneous QuickBird or other imagery with visual and near-infrared bands at the m-scale. The entire procedure is operational and can be applied anywhere simultaneous imagery of Landsat and QuickBird or similar imagery is available.

Future work will need to focus on: 1. Evaluation of the best and most simple stratification procedures to predict root zone soil moisture at m-scale from Landsat satellite imagery; 2. A field validation of the downscaling approach in the Middle Rio Grande Valley of New Mexico using it as a proxy for Helmand Province in Afghanistan. These activities are best done by a two year post-doc or four year PhD graduate student effort.

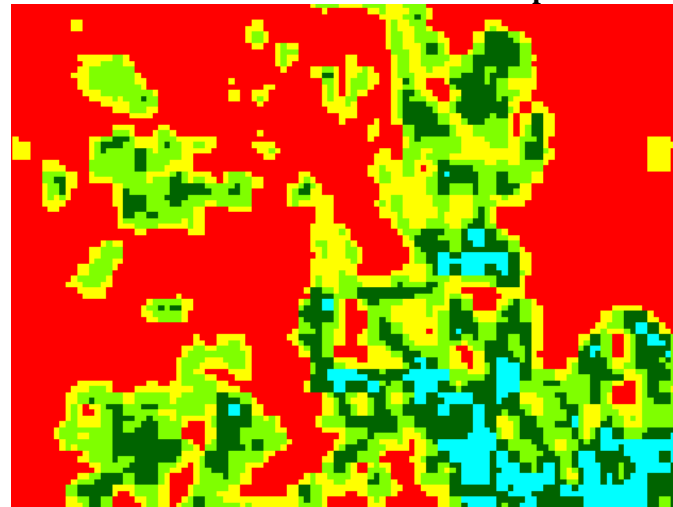
7. ACKNOWLEDGEMENT

This research has been funded by the Coastal and Hydraulics Laboratory, Engineer Research and Development Center of the U.S. Army Corps of Engineers in Vicksburg, MS. Part of the funding consisted of a STIR grant that was managed through the Army Research Office. The Quickbird imagery was kindly provided by the Army Geospatial Center, Engineer Research and Development Center of the U.S. Army Corps of Engineers in Fort Belvoir, VA.

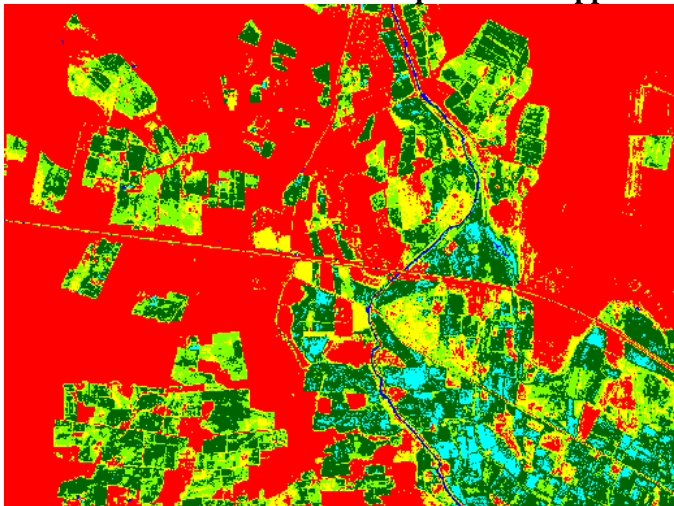
QuickBird Image



Landsat Soil Moisture Map



Downscaled Soil Moisture Map – Global Approach



Downscaled Soil Moisture Map – Stratification Approach

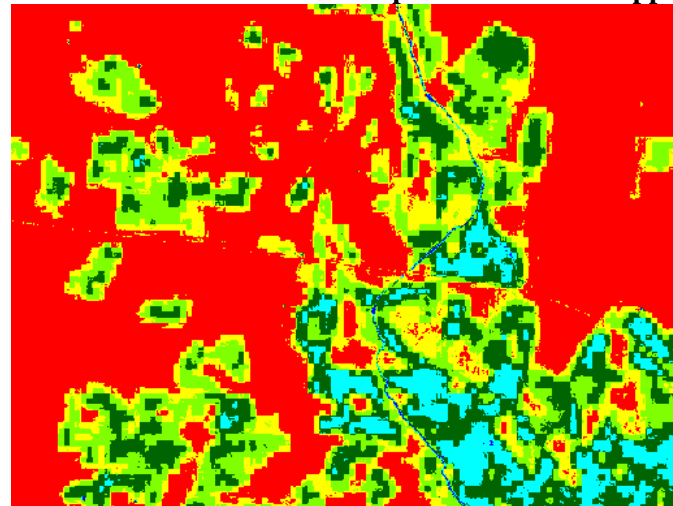
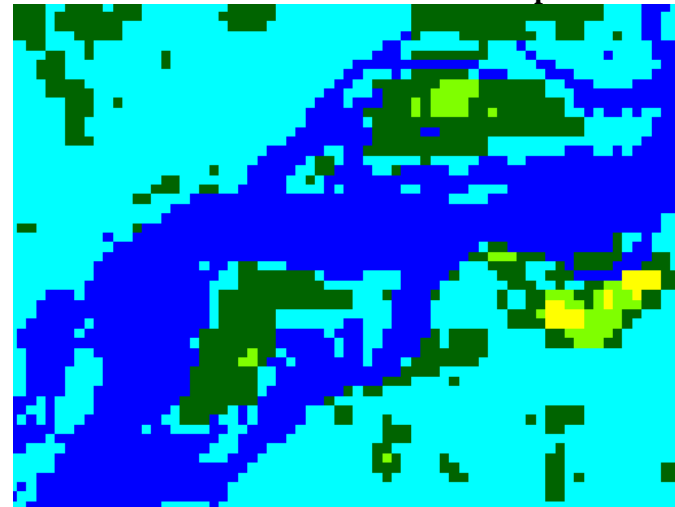


Figure 7. The dry hot asphalt road shows up at an elevated moisture content (yellow/light green) in the Global Approach but has almost disappeared in the Stratification Approach.

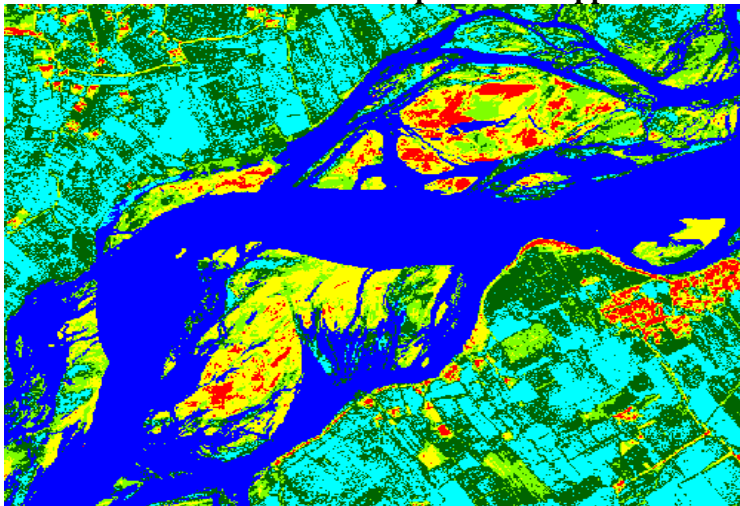
QuickBird Image



Landsat Soil Moisture Map



Downscaled Soil Moisture Map – Global Approach



Downscaled Soil Moisture Map – Stratification Approach

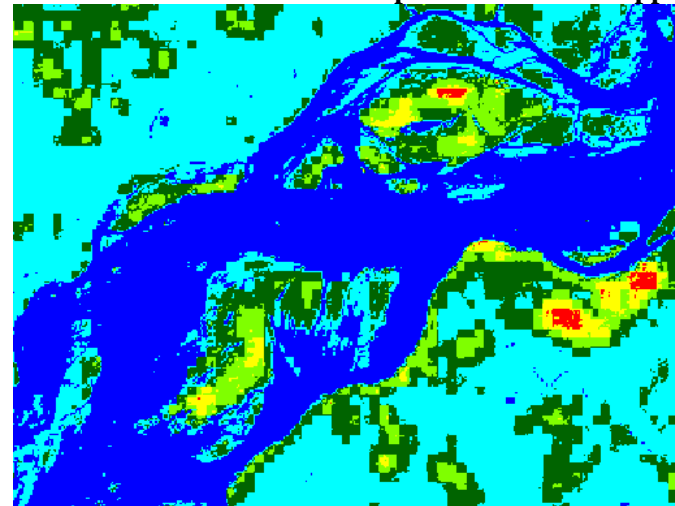


Figure 8. The moist cool sandbanks in the river show up with a very low moisture content (red) in the Global Approach but have higher soil moisture contents (light green, and green) in the Stratification Approach.

REFERENCES

1. Lessem, A., G. Mason, and R. Ahlvin, *Stochastic vehicle mobility forecasts using the NATO reference mobility model*. Journal of Terramechanics, 1996. **33**(6): p. 273-280.
2. Van Dam, R.L., et al., *Environmental effects on landmines and UXO detection sensors*. Fast Times, 2005. **10**(1): p. 36.
3. Van Dam, R.L., B. Borchers, and J.M.H. Hendrickx, *Soil effects on thermal signatures of buried nonmetallic landmines*. Proc. International Society for Optical Engineering, SPIE, 2003. **5089**: p. 1210-1218.
4. Miller, T.W., J.M.H. Hendrickx, and B. Borchers, *Radar detection of buried landmines in field soils*. Vadose Zone J, 2004. **3**: p. 1116-1127.
5. Miller, T.W., et al., *Effect of soil moisture on land mine detection using ground penetrating radar*. Proc. International Society for Optical Engineering, SPIE, 2002. **4742**: p. 281-290.
6. Hong, S.-H., et al., *Land mine detection in bare soils using thermal infrared sensors*. Proc. International Society for Optical Engineering, SPIE, 2002. **4742**: p. 43-50.
7. Hong, S.-H., et al., *Impact of soil water content on landmine detection using radar and thermal infrared sensors*. Proc. International Society for Optical Engineering, SPIE, 2001. **4394**: p. 409-416.
8. Das, B.S., J.M.H. Hendrickx, and B. Borchers, *Modeling transient water distributions around landmines in bare soils*. Soil Science, 2001. **166**(3): p. 163-173.
9. Borchers, B., et al., *Enhancing dielectric contrast between land mines and the soil environment by watering: modeling, design, and experimental results*. Proc. International Society for Optical Engineering, SPIE, 2000. **4038**(2): p. 993-1000.
10. Hendrickx, J.M.H., et al., *Worldwide distribution of soil dielectric and thermal properties*. Proc. International Society for Optical Engineering, SPIE, 2003. **5089**: p. 1158-1168.
11. Niedzialek, J.M. and F.L. Ogden, *Numerical investigation of saturated source area behavior at the small catchment scale*. Adv. Water Resour., 2004. **27**: p. 925-936.
12. Downer, C.W., et al., *Theory, development, and applicability of the surface water hydrologic model CASC2D*. Hydrological Processes, 2002. **16**(2): p. 255-275.
13. Senarath, S.U.S., et al., *On the calibration and verification of distributed, physically-based, continuous, Hortonian hydrologic models*. Water Resour. Res., 2000 **36**(6): p. 1495-1510.
14. Downer, C.W. and F.L. Ogden, *Users Manual: Gridded Surface/Subsurface Hydrologic Analysis*, in *Engineering Research and Development Center Technical Report*. 2003, U.S. Army Corps of Engineers.
15. Downer, C.W. and F.L. Ogden, *GSSHA: A model for simulating diverse streamflow generating processes*. J. Hydrol. Engrg., 2004. **9**: p. 161-174.
16. Dingman, S.L., *Physical Hydrology. Second Edition*. 2002, Upper Saddle River, New Jersey 07458: Prentice Hall. 646.
17. Ogden, F.L., et al., *Hydrologic analysis of the Fort Collins, Colorado, flash flood of 1997*. J. Hydrology, 2000. **228**: p. 82-100.
18. Shukla, J. and Y. Mintz, *Influence of land surface evapotranspiration on the earth's climate*. Science, 1982. **215**: p. 1498-1501.
19. Milly, P.C.D. and K.A. Dunne, *Sensitivity of the global water cycle to the water-holding capacity of land*. J. Climate, 1994. **7**: p. 506-526.
20. Van de Hurk, B.J.J.M., W.G.M. Bastiaanssen, H. Pelgrum, and E. van Meijgaard, *A new methodology for assimilation of initial soil moisture fields in weather prediction models using Meteosat and NOAA data*. Journal of Applied Meteorology, 1997. **36**: p. 1271-1283.
21. Ryerson, C.C., et al., *Field Data Archive. Report Number A494305*. 2008, ENGINEER RESEARCH AND DEVELOPMENT CENTER HANOVER NH COLD REGIONS RESEARCH AND ENGINEERING LAB. p. 18.
22. Davis, A., *The use of commercial remote sensing in predicting helicopter brownout conditions*. 2007, Naval Postgraduate School Monterey CA. p. 93.
23. McWilliams, G. *Preparing for NPOESS: a new era of environmental satellite data*. 2003 October 16, 2005 [cited; Available from: <http://www.nrlmry.navy.mil/BACIMO/2003/proceedings/4-07%20McWilliams.doc>].
24. McWilliams, G., et al., *Analysis of the enhanced tactical utility of NPOESS soil moisture data using combat simulations - Draft*. 2003, Adelphi, MD 20783: Army Research Laboratory. 55.
25. Van Dam, R.L., B. Borchers, and J.M.H. Hendrickx, *Strength of landmine signatures under different soil conditions: implications for sensor fusion*. International Journal of Systems Science, 2005. **36**(9): p. 573-588 DOI: 10.1080/00207720500147800
26. Hendrickx, J.M.H., et al., *Soil effects on ground penetrating radar (GPR) detection of buried non-metallic mines.*, in *Ground Penetrating Radar: Applications in Sedimentology*, C.S. Bristow and H.M. Jol, Editors. 2003, Geological Society: London, U.K. p. 191-198.
27. Hendrickx, J.M.H., et al., *Improvement of hydrologic model soil moisture predictions using SEBAL evapotranspiration estimates*. Proc. International Society for Optical Engineering, SPIE, 2009. **7303**: p. 730311.
28. Fleming, K., J.M.H. Hendrickx, and S.-h. Hong, *Regional mapping of root zone soil moisture using optical satellite imagery*. Proc. International Society for Optical Engineering, SPIE, 2005. **5811**: p. 159-170.
29. Hendrickx, J.M.H., et al., *Mapping energy balance fluxes and root zone soil moisture in the White Volta Basin using optical imagery*. Proc. International Society for Optical Engineering, SPIE, 2006. **6239**: p. 238-249.
30. Hendrickx, J.M.H., et al., *High-resolution soil moisture mapping using operational optical satellite imagery*. Proc. International Society for Optical Engineering, SPIE, 2010. **7664**: p. 7303 - 91.
31. Howington, S.E., *Soil moisture and heat transport modeling to support simulation of infrared imaging*. Abstract., in *8th. World Congress on Computational Mechanics (WCCM8) & 5th European Congress on Computational Methods in Applied Sciences and Engineering (ECCOMAS 2008)*. 2008: Venice, Italy.
32. Howington, S.E., et al., *A model to simulate the interaction between groundwater and surface water*, in *1999 High-Performance Computing Users Group Meeting*. 1999, Washington, DC: DoD HPC Modernization Office: Monterey, CA.
33. Howington, S.E., et al., *A Suite of Models for Producing Synthetic, Small-Scale Thermal Imagery of Vegetated Soil Surface*, in *XVI International Conference on Computational Methods in Water Resources*, P.J. Binning, et al., Editors. 2006: Copenhagen, Denmark.

34. Owe, M. and A.A. van de Griend, *Daily surface moisture model for large area semi-arid land applications with limited climate data*. J. Hydrology, 1990. **121**: p. 119-132.
35. Kustas, W.P., X. Zhan, and T.J. Jackson, *Mapping surface energy flux partitioning at large scales with optical and microwave remote sensing data from Washita '92*. Water Res. Res., 1999. **35**(1): p. 265-277.
36. De Bruin, H.A.R., *A model for the Priestley-Taylor parameter alpha*. J. Clim. Appl. Meteorol., 1983. **22**: p. 572-578.
37. Davies, J.A. and C.D. Allen, *Equilibrium, potential and actual evapotranspiration from cropped surfaces in southern Ontario*. J. Appl. Meteorol., 1973. **12**: p. 649-657.
38. Scott, C.A., W.G.M. Bastiaanssen, and M.-u.-D. Ahmad, *Mapping Root Zone Soil Moisture Using Remotely Sensed Optical Imagery*. J. Irrig. and Drain. Engrg., 2003. **129**(5): p. 326-335.
39. Bastiaanssen, W.G.M., et al., *Area-averaged estimates of evaporation, wetness indicators and top soil moisture during two golden days in EFEDA*. Agric. For. Meteorol., 1997. **87**(2-3): p. 119-137.
40. Ahmad, M.-u.-D. and W.G.M. Bastiaanssen, *Retrieving soil moisture storage in the unsaturated zone using satellite imagery and bi-annual phreatic surface fluctuations*. Irrigation and Drainage Systems, 2003. **17**(3): p. 141-161 doi:10.1023/A:1025101217521.
41. Hong, S.-h., J.M.H. Hendrickx, and B. Borchers, *Effect of scaling transfer between evapotranspiration maps derived from LandSat 7 and MODIS images*. Proc. International Society for Optical Engineering, SPIE, 2005. **5811**: p. 147-158.
42. Hendrickx, J.M.H. and S.-h. Hong, *Mapping sensible and latent heat fluxes in arid areas using optical imagery*. Proc. International Society for Optical Engineering, SPIE, 2005. **5811**: p. 138-146.
43. Bastiaanssen, W.G.M., et al., *A remote sensing surface energy balance algorithm for land (SEBAL). Part 2: Validation*. Journal of Hydrology, 1998. **212-213**: p. 213-229.
44. Bastiaanssen, W.G.M., et al., *SEBAL model with remotely sensed data to improve water-resources management under actual field conditions*. J. Irrig. and Drain. Engrg., ASCE, 2005. **131**(1): p. 85-93.
45. Bastiaanssen, W.G.M., et al., *A remote sensing surface energy balance algorithm for land (SEBAL): Part 1. Formulation*. Journal of Hydrology, 1998. **212-213**: p. 198-212.
46. Wagenet, R.J. and J.L. Hutson, *Scale-dependency of solute transport modeling/GIS applications*. J. of Environmental Quality, 1996. **25**: p. 499-510.
47. Feddes, R.A., P.J. Kowalik, and H. Zaradny, *Simulation of field water use and crop yield*. Simulation Monographs. 1978, Wageningen, The Netherlands: Pudoc.
48. Feddes, R.A., et al., *Modelling soil water dynamics in the unsaturated zone - state of the art*. J. Hydrology, 1988. **100**: p. 69-111.
49. Belmans, J.G., J. Wesseling, and R.A. Feddes, *Simulation of the water balance of a cropped soil, SWATRE*. J. of Hydrology 1983. **63**: p. 271-286.
50. Allen, R.G., *Using the FAO-56 dual crop coefficient method over an irrigated region as part of an evapotranspiration intercomparison study*. J. of Hydrology, 2000. **229**: p. 27-41.
51. Crago, R.D., *Conservation and variability of the evaporative fraction during the daytime*. J. of Hydrol., 1996. **180**: p. 173-194.
52. Brutsaert, W. and M. Sugita, *Application of self-preservation in the diurnal evolution of the surface energy budget to determine daily evaporation*. J. of Geophysical Res., 1992. **97:D17**: p. 18,377-18,382.
53. Boni, G., D. Entekhabi, and F. Castelli, *Land data assimilation with satellite measurements for the estimation of surface energy balance components and surface control on evaporation*. Water Res. Res., 2001. **37**(6): p. 1713-1722.
54. Smith, E.A., et al., *Area-averaged surface fluxes and their time-space variability over the FIFE experimental domain*. J. of Geophysical Res., 1992. **97(D17)**: p. 18,599-18,622.
55. Bolle, H.-J., et al., *EFEDA: European field experiment in a desertification-threatened area*. Ann. Geophys., 1993. **11**: p. 173-189.
56. Allen, R.G., M. Tasumi, and R. Trezza, *Satellite-based energy balance for mapping evapotranspiration with internalized calibration (METRIC) - Model*. Journal of Irrigation and Drainage Engineering, 2007. **133**: p. 380-394.
57. Bastiaanssen, W.G.M., D.J. Molden, and I.W. Makin, *Remote sensing for irrigated agriculture: examples from research and possible applications*. Agricultural Water Management, 2000. **46**(2): p. 137-155.
58. Boettinger, J.L., et al., eds. *Digital soil mapping. Bridging research, production, and environmental application*. 2010, Springer. 473.
59. Campbell, J.B., *Introduction to Remote Sensing, Fourth Edition*. 2007, New York, NY: The Guilford Press. 627.